Experimental and Analytical Investigation on Flexural Retrofitting of RC T-Section Beams Using CFRP Sheets

Yannian Zhang [1,2] **and Moncef L. Nehdi** [1,*]

[1] Department of Civil and Environmental Engineering, Western University, London, ON N6A 5B9, Canada
[2] School of Civil Engineering, Shenyang Jianzhu University, Shenyang 110168, China; zyntiger@163.com
*   Correspondence: mnehdi@uwo.ca

check for updates

Abstract: The large portfolio of aging highway bridges worldwide includes many reinforced concrete T-section beams with various levels of damage and degradation. However, there is currently dearth of research on the anchoring behavior of CFRP sheets used for strengthening such RC T-section beams. Moreover, there is a need for rational and accurate analytical models to predict the strengthening effect of CFRP sheets for RC T-section beams. In this study, eight RC T-section beam specimens strengthened with externally bonded CFRP sheets were tested under quasi-static loading. The failure mode, cracking resistance, yielding and ultimate capacity were examined. The effects of U-wrap spacing, flexural reinforcing ratio, and concrete compressive strength on the flexural behavior of the CFRP strengthened RC T-section beams were analyzed and discussed. New analytical models were developed to predict the cracking, yielding and ultimate load resistance of the RC T-section beams strengthened with CFRP sheets. The analytical models were validated through comparing its predictions with experimental results, and they demonstrated adequate accuracy. The findings could be deployed for the retrofitting of a large portfolio of aging highway bridges with deteriorated reinforced concrete T-section beams.

Keywords: highway bridges; reinforced concrete; T-section beam; retrofitting; CFRP; flexural behavior

1. Introduction

Many bridges serve under harsh environmental and mechanical loading conditions. Due to population growth and urbanization, traffic flow has increased substantially over the last few decades, while vehicle loads have gradually increased. Accordingly, many bridges have become structurally deficient or obsolete [1]. Thus, deploying various strengthening schemes to extend the service life of bridges has attracted greater interest [2] and has become a major challenge for modern civil engineering [3].

Owing to simple construction and relatively lower cost, T-section beams have been extensively used in highway bridges around the world. In service, such T-section beams can be subjected to chloride ions ingress, carbonization and moisture intrusion, ultimately causing corrosion of the reinforcing steel, cracking, spalling and delamination. Such damage mechanisms compromise the load carrying capacity of the T-section beams and shortening the service life of the bridge. Previous studies indicated that strengthening these T-section beams is generally more economical and sustainable compared to its replacement [4]. Thus, strengthening T-section beams has become a primary concern in improving the structural performances of bridges with T-section beams.

In recent years, using fiber-reinforced polymer (FRP) materials for strengthening concrete structures experienced very rapid growth around the world [5], particularly in cases of design code changes,

deficient design, construction flaws, or structural degradation due to environmental exposure, natural hazards or excessive loading [6]. Externally bonded FRP reinforcement has proven especially effective for strengthening RC beams owing to its light-weight, excellent durability, and rapid installation. Yet, premature failure for instance due de-bonding can limit the system effectiveness, leading to possible brittle modes that can deter designers from exploring the full potential of this material [7].

In FRP-strengthened beams, failure may occur due to beam shear, flexural compression, FRP rupture, FRP debonding, or concrete cover ripping [8,9]. CFRP was used for strengthening RC structures in lieu of traditional steel plate strengthening techniques. For instance, Badawi et al. [10] and Al-Mahmoud et al. [11] studied the flexural strength of RC beams with prestressed CFRP rods experimentally and analytically. Yost et al. [12] reported experimental studies on the flexural behavior of RC beams strengthened by CFRP strips. Bilotta et al. [13], Barros and Fortes [14] and Nanni et al. [15] investigated the flexural and shear strength of beams or girders strengthened with CFRP. Most existing experimental and analytical studies focused on the structural performance of RC members with externally bonded CFRP sheets or strips. However, there is currently little published work on the anchoring for RC T-Section beams strengthened with CFRP sheets, along with a lack of studies on the influence of CFRP U-wrap spacing on anchorage and mechanical properties. Comparative studies on the bonding efficiency of this strengthening technique are still limited. Additionally, rational and accurate analytical models considering the above parameters are scarce.

The present study reports the findings of a test program on eight RC T-section beams reinforced with CFRP sheets tested to failure under two-point loading. The flexural performance of the T-section beams is explored, and the effects of influential parameters, including concrete compressive strength, reinforcing steel ratio, thickness of the strengthening material, and spacing of the strengthening U-wraps are discussed and analyzed. Based on the test results, a predictive analytical model was developed and recommendations for selection of CFRP sheets on T-section beams are formulated.

2. Research Significance

There is currently dearth of published research on the anchoring of CFRP sheets used to strengthen RC T-Section beams, along with lack of studies on the influence of CFRP U-wrap spacing and other key parameters on anchorage and overall mechanical properties. Comparative studies on the bonding efficiency of this strengthening technique are still limited. Additionally, rational and accurate analytical models considering the key influential parameters are still scarce. In this study, this knowledge gap is addressed via testing eight RC T-section beam specimens strengthened with externally bonded CFRP sheets. The experimental findings on the failure mode, cracking resistance, yielding and ultimate capacity, and on the effects of U-wrap spacing, flexural reinforcing ratio, and concrete compressive strength on the flexural behavior of the CFRP strengthened RC T-section beams should guide the practical retrofitting of such beams in the large portfolio of ageing bridges. The new analytical models developed to predict the cracking, yielding and ultimate load resistance of the RC T-section beams strengthened with CFRP sheets should provide a useful tool with adequate predictive accuracy to help engineers design suitable retrofit schemes for such beams.

3. Test Program

3.1. Materials Properties and Test Specimens

The materials used in this test program include CFRP sheets, C20 and C40 normal-weight portland cement concrete, Ø8 mm HPB235 shear reinforcement, Ø12 mm and Ø14 mm flexural reinforcement, JGJ-20 adhesive. The used CFRP is TORAY-T700-12K type CFRP with thickness of 0.167 mm. All tested RC beams were cast at the same time. The compressive strength of two grades of concrete C20 and C40 were 21.3 MPa and 42.7 MPa, as determined by on cubic samples at the age of 28 days. Table 1 summarizes the details of the tested T-section beam specimens. Both C20 and C40 concrete was used to study the influence of the concrete compressive strength on the anchorage performance of

CFRP Sheets. Moreover, the reinforcement ratio was 0.95% and 1.29% to gain insight into its effect on the reinforcing efficiency of CFRP sheets. Single and double CFRP layers were used to explore the influence of the bonding layers on the anchorage performance of CFRP sheets. Furthermore, the CFRP U-wrap spacing was 100 mm and 150 mm to investigate its effect on the anchorage of CFRP sheets. Table 2 lists the mechanical properties of the materials used in this test program, while Table 3 lists the mechanical properties of the CFRP and adhesive. Eight T-section beam specimens were prepared in this test program, measuring $90 \times 290 \times 2100$ mm in web-width, depth, and length, respectively. The thickness and width of the flange of the T-section beam were 60 mm and 400 mm, respectively. The CFRP sheets were attached to the bottom of the T-section beams by JGJ-20 type constructional adhesive material. Three specimens (B1, B2 and B3) were not strengthened, while five specimens (C1 to C5) were strengthened using surface bonded CFRP sheets. Ø12 mm HRB335 hot rolled steel rebar was used as compressive reinforcement. Ø12 mm and Ø14 mm HRB335 hot rolled steel rebar was used as tensile reinforcement, representing flexural reinforcing ratios of 0.95% and 1.29%, respectively. The shear reinforcement adopted Ø8 mm HPB235 hot rolled steel reinforcement. Figure 1a shows the reinforcement details for the T-section beams. CFRP sheets were first installed at the bottom surface of the T-section beams, then CFRP U-wraps sheets were attached to the T-section beams using epoxy cohesive. Figure 1b illustrates the layout of U-wraps along the length of the beam. Figure 1c displays the size of the cross-section of the T-section beams. The main parameters studied were the compressive strength of concrete, reinforcing ratio, layers of the CFRP strengthening, and spacing of CFRP U-wraps.
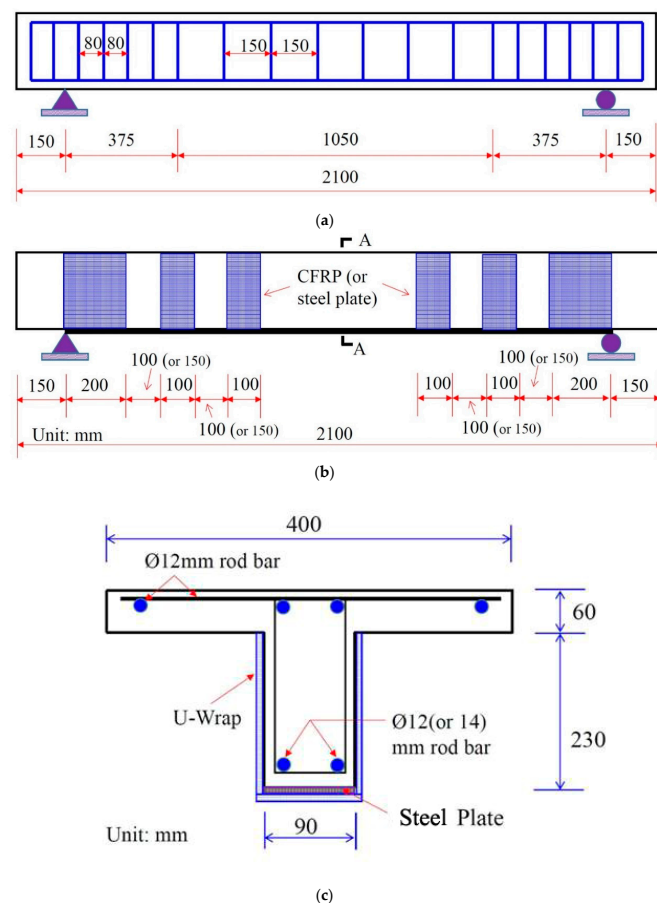

Figure 1. Details of tested T-section beams. (**a**) Layout of reinforcement in the T-beam. (**b**) Layout of CFRP type of U-wrap. (**c**) A-A section for T-beam.

Table 1. Details and test results of T-section beams retrofitted with CFRP sheets.

Item	Conc Grade	ρ_{fl} (%)	Bonding Layers	S (mm)	u_y (mm)	u_{max} (mm)	$P_{cr,T}$ (kN)	$P_{y,T}$ (kN)	$P_{u,T}$ (kN)	Failure Mode	P_{cr} (kN)	$P_{cr,T}/P_{cr}$ ratio	P_y (kN)	$P_{y,T}/P_y$ Ratio	P_u (kN)	$P_{u,T}/P_u$ Ratio
B1	C20	0.95	-	-	6.6	49.2	8.7	29.9	44.9	FB	7.7	1.13	24.7	1.21	37.7	1.19
B2	C40	0.95	-	-	7.1	60.0	9.3	29.5	45.4	FB	10.7	0.87	26.5	1.11	38.0	1.20
B3	C20	1.29	-	-	8.0	44.2	7.5	46.2	61.4	FB	7.9	0.95	34.6	1.33	52.7	1.17
C1	C20	0.95	1	100	6.6	51.2	9.2	42.6	47.5	FB&DB	7.8	1.07	38.7	1.10	50.1	0.95
C2	C40	0.95	1	100	7.3	20.0	9.0	41.9	50.5	FB&DB	10.8	0.94	39.2	1.07	51.1	0.99
C3	C20	1.29	1	100	7.8	19.0	8.2	48.2	70.5	FB&DB	8.0	1.20	46.9	1.03	62.2	1.13
C4	C20	0.95	2	100	7.3	15.5	11.4	48.5	66.6	FB&DB	7.8	1.09	54.4	0.89	67.6	0.99
C5	C20	0.95	1	150	6.5	20.5	9.7	42.0	51.0	FB&DB	7.8	0.90	38.7	1.08	50.1	1.02
Mea												1.01		1.10		1.08
Cov												0.12		0.12		0.10

S denotes spacing of the U-wrap; *DB* denotes debonding failure; *FB* denotes flexural bending failure; *Mea* denotes mean value; *Cov* denotes coefficient of variation.

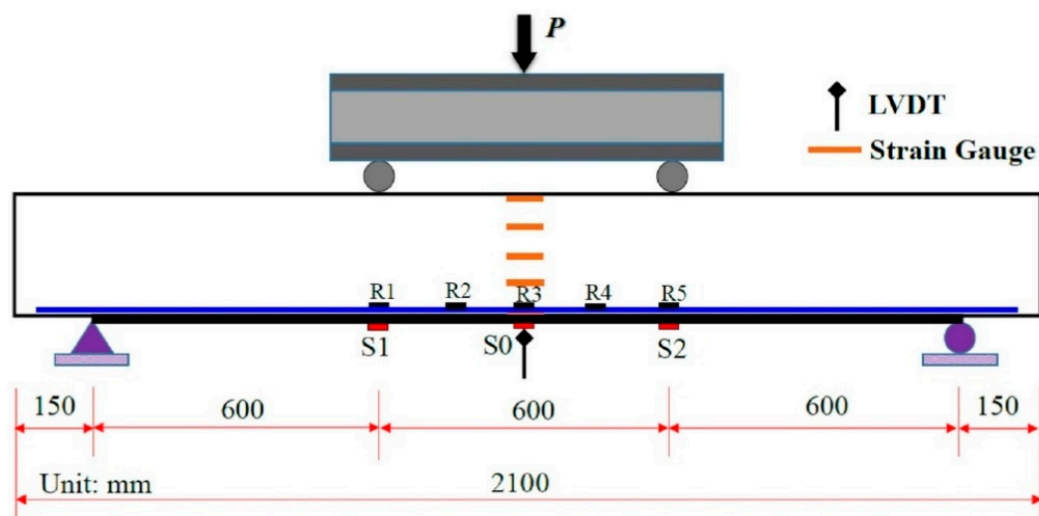**Table 2.** Details of materials involved in test program.

Type	E_s (GPa)	f_y (MPa)	F_u (MPa)	δ_u (%)
Ø8 HPB235	200	308	538	30.5
Ø12 HRB335	200	365	550	28.5
Ø14 HRB335	200	388	605	27.5

Table 3. CFRP and cohesive materials.

Type	f_y (MPa)	E_F (GPa)	δ_u (%)	τ_c (MPa)
CFRP	3168	242	1.71	3.5
JGJ-20	43	2.59	-	3.6

3.2. Test Setup and Procedures

Figure 2 shows the test setup for the T-section beam specimens. T-section beams were simply supported with a span of 1800 mm. Displacement controlled loading was applied to the beam at 1/3 and 2/3 span of the beam. Linear varying displacement transducers (LVDTs) were installed at the mid-span to record central deflections of the T-section beams at different loading levels. A load cell was used to measure the reaction forces acting on the beams. To measure strain distribution along the cross-section of the T-section beams, five linear strain gauges (R_1–R_5) were installed on the concrete surface with equal spacing along the depth of the cross-section at mid-span. Five linear strain gauges were also installed on the main flexural reinforcement with equal spacing to record strains developed in the reinforcing steel during the testing process. Three linear strain gauges were also attached to the strengthening CFRP at the bottom of the T-section beams.

Figure 2. Test setup and measurements on T-section beams.

4. Experimental Test Results

4.1. General Behavior

Figure 3 shows the load versus central deflection curves for the tested RC T-section beam specimens strengthened by CFRP sheets. It can be observed that there are three stages. The first is the elastic stage that started with initial loading until the first crack developed in the bottom tensile fiber at mid-span. The resistance of the T-section beam corresponds to the concrete cracking is denoted P_{cr} (Figure 3a). Subsequently, in the stage II, the applied load was redistributed. Both strains in the main flexural reinforcement and CFRP sheet increased rapidly. At the end of this stage, the RC T-section beam behaved elastically and reached it yield strength, P_y (Figure 3a). $\boldsymbol{P_{cr}}$ was improved significantly

when bonding layers increased. However, it showed obvious brittle failure (Figure 3a,b). Figure 4a,b illustrate the strain versus resistance curves of the main flexural reinforcement and CFRP sheet at mid-span, respectively. It can be observed that the flexural reinforcement reached its yielding strain. The stiffness of the beam in stage II was smaller than that in stage I due to flexural cracking of the T-section beam. Figure 5a–f display the observed cracks due to the flexural bending moment. In stage III, there were two distinct structural behaviors for the tested specimens. Beams B1~B3 exhibited ductile behavior, whilst the T-section beams strengthened with CFRP sheets exhibited sudden drop in P-δ curves as shown in Figure 3. This implies that different types of failure modes occurred in the test specimens with and without CFRP-strengthening.
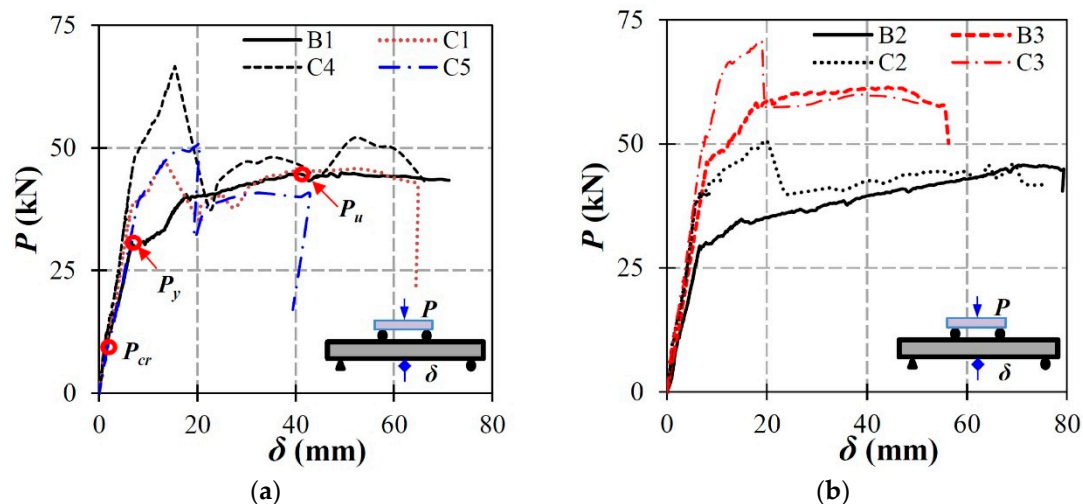

Figure 3. Load-central deflection curves of RC T-section beams retrofitted by CFRP. (**a**) *P*-δ curves for B1, C1, C4-5; (**b**) P-δ curves for B2-3, C2-3.
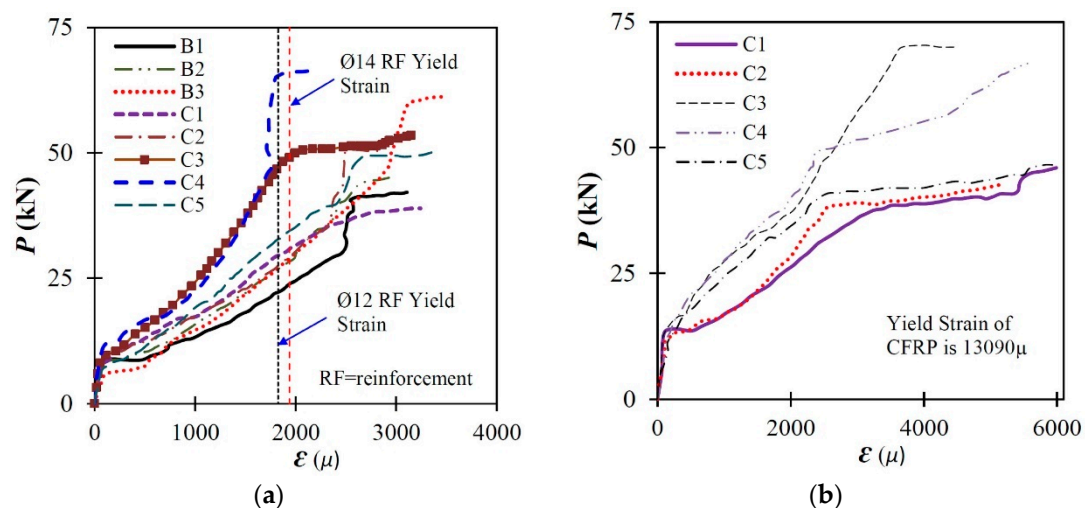

Figure 4. Load-strain curves of RC T-section beams retrofitted by CFRP. (**a**) Strain in steel reinforcement at mid-span; (**b**) Strain in CFRP at mid-span.

Figure 5. Cracks developed in RC T-section beams strengthened by CFRP. (**a**) B1 (**b**) B2. (**c**) B3 (**d**) C1. (**e**) C2 (**f**) C3. (**g**) C4 (**h**) C5.

4.2. Load Resistance and Failure Modes

The cracking resistance P_{cr}, resistance corresponding to steel yielding P_y, and ultimate resistance P_u of the tested T-section beams could be determined from P-δ curves of beams as shown in Figure 3. Table 1 lists the P_{cr}, P_y, and P_u values and the corresponding failure mode for each of the tested 8 T-section beam specimens. Based on the P-δ curves and load-strain curves of the main steel reinforcement and CFRP, two distinct failure modes were observed. The first is a flexural mode that occurred in beams B1~B3, which was characterized by: (1) strength hardening plateau of the P-δ curves; (2) yielding of the bottom steel reinforcement at final failure (Figure 4a); and (3) flexural cracks at the pure bending region in the T-section beam (Figure 5). The combined flexural failure and CFRP-concrete debonding failure occurred in beams C1~C5 at final failure stage. This was accompanied by: (1) much smaller strains of about 6000μ in the CFRP than failure strain of 13090μ, which implies that the CFRP did not fail in tension; (2) yielding of the bottom steel reinforcement at final failure (Figure 4a); and (3) step drops in the P-δ curves of specimens C1~C5. $\boldsymbol{P_{cr}}$ and P_y increased significantly when bonding layers increased (C4) or the reinforcement ratio increased (C3). However, peeling failure often occurred when there was excessive bonding of FRP.The peeling of the CFRP from the bottom of the T-section beam specimens was evident in C4 (Figure 5).

4.3. Effect of Different Parameters

Figure 6 shows the effect of different parameters on the resistance of the RC T-section beams strengthened with CFRP. The cracking resistance Pcr was not significantly affected by the number of CFRP layers. However, increasing the flexural reinforcing ratio ρf ρ_{fl} from 0.95% to 1.29%, decreasing U-wrap spacing from 150 mm to 100 mm, and increasing the compressive strength of concrete from 20 MPa to 40 MPa increased the Pcr value by 16%, 19%, and 23%, respectively. Using higher strength concrete leads to higher cracking tensile strength of the beam as expected. Also, increasing the flexural reinforcing ratio offers larger equivalent cross-section area; and decreasing the spacing of the CFRP U-rap increases the stiffness of the beam, which delays the cracking of the concrete. As the number of CFRP sheets increased from 0 to 1 and 2, the Py (or Pu) values increased by 42% (or 6%) and 62% (or 48%), respectively. This is because introducing CFRP sheets to RC T-section beams increases the equivalent reinforcing ratio of the beam, which contributes to their Py and Pu resistance. However, the CFRP-concrete bonding failure limits the full utilization of the CFRP, which is reflected in the much lower than the strain at failure of the T-section beams. Hence, peeling of the CFRP from the strengthened RC T-section beams needs further study. Increasing the flexural reinforcing ratio of the T-section beam, ρ_{fl} from 0.95% to 1.29% led to 13% and 48% increments in Py and Pu, respectively. Increasing the flexural reinforcing ratio of the T-section beams increases the bending moment resistance of the cross-section. Due to premature failure of the CFRP-concrete bonding, the contribution of the CFRP to the bending resistance is minimized.
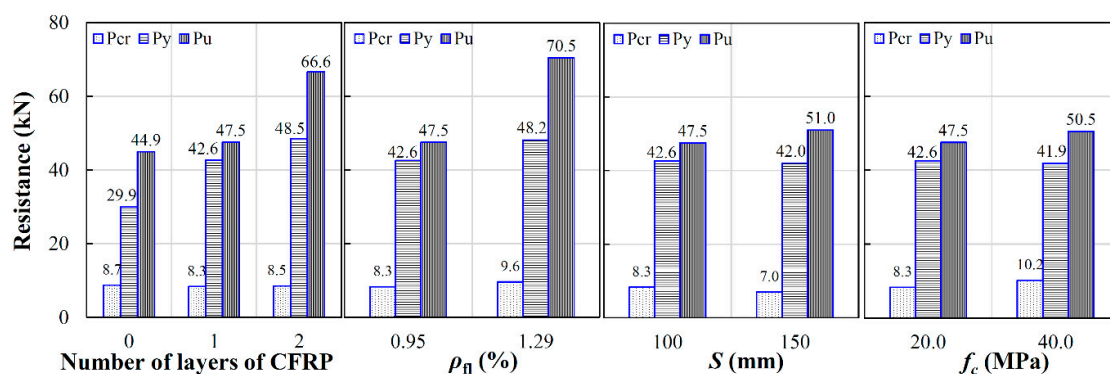

Figure 6. Effects of different parameters on resistance of RC T-beam strengthened by CFRP.

Increasing the spacing of the CFRP U-wrap, S, had limited effect on *Py* and *Pu*. As the spacing of the CFRP U-wrap increased from 100 mm to 150 mm, the *Py* and Pu values only changed by -1% and 7%, respectively. This is likely because all tested specimens failed in a flexural mode, and the spacing of the U-wrap only increases the transverse shear resistance of the T-section beam without improvement on its flexural bending resistance. The test results also show that using higher strength concrete had limited influence on the flexural resistance of the RC T-section beams strengthened with CFRP. This may be caused by the CFRP-concrete bonding failure of the beam.

5. Discussion

From the above test results, it can be deduced that CFRP sheets can improve the flexural resistance of the RC T-section beam specimens. The efficiency of the CFRP sheet strengthening regarding the resistance of RC T-section beams was evaluated as follows:

$$\overline{P}_u = \frac{\Delta P_u}{P_{yT}} \tag{1}$$

$$P_T = f_{yr} A_r \tag{2}$$

where P_{yT} and P_u denote the yielding and ultimate resistance of the T-section beam; P_T denotes tensile resistance of the strengthening materials; f_{yr} and A_r denote the yield strength and cross-sectional area of the strengthening CFRP sheet, respectively. In Equation (1) higher $\overline{P}_u$ values denote improved resistance of the beam by unit strength of strengthening sheets. Figure 7 shows the $\overline{P}_u$ values for the strengthened specimens. The effect of premature failure of the bonding glue that connects the CFRP to the T-section beams can be noted. As can be observed in Figure 4, all strengthened CFRP materials did not reach maximum strain at the failure stage of strengthened beam specimens.
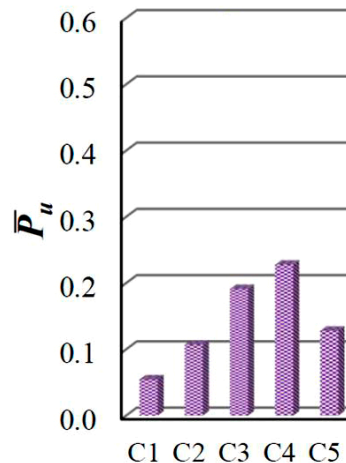

Figure 7. $\overline{P}_u$ values for strengthened T-section beam specimens.

Figure 8 shows the central deflections, u_{max} of the tested T-section beam specimens at their ultimate resistance, P_u. Central deflections were increased on average by 20% from 50 mm to 60 mm compared with that of the un-strengthened T-section beams. However, the ductility of the T-section beams strengthened by CFRP was decreased due to premature failure of the bonding materials. The average central deflection of beams strengthened by CFRP sheets was about 20 mm, which is only 40% of that for the un-strengthened beams.
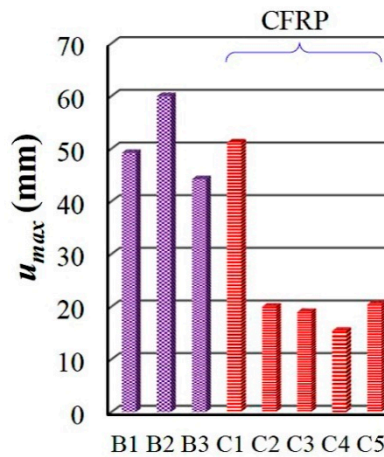
Figure 8. Central deflections u_{max} of tested T-section beam specimens at ultimate resistance.

6. Ultimate Load Carrying Capacity of strengthened T-Section Beams

6.1. Resistance of T-Section Beams Corresponding to Crack Initiation P_{cr}

The bending resistance of the RC T-section beams corresponding to the tensile crack initiation of cross-section can be obtained through solving the position of the neutral axis, x, as shown in Figure 9. The assumptions made include: (1) plane sections remain plane; (2) the ultimate tensile stress of the concrete was achieved at the bottom fiber of the cross-section; (3) the strengthening materials had perfect bond with the T-section beams and no bonding failure occurred. Setting the resultant forces acting on the section equal to zero, x can be solved as follows;

$$N_{cc} + N_{sc} = N_{st} + N_{ct} + N_r \tag{3}$$

$$N_{cc} = \begin{cases} 0.5E_c\epsilon_c\left[\left(1 + \frac{x-h_1}{x}\right)B_f h_t + \frac{(x-h_t)^2}{x}b\right] \\ 0.5E_c\epsilon_c B_f h_t \end{cases} \qquad \begin{bmatrix} for \quad x > h_t \\ \\ for \quad x \leq h_t \end{bmatrix} \tag{4}$$

$$N_{cs} = A_{sc}E_s\epsilon_{cs} \tag{5}$$

$$N_{ct} = \begin{cases} 0.5E_c\epsilon_{ct}b(h-x) \\ 0.5E_c\epsilon_{ct}\left\{\frac{(h_t-x)^2}{h-x}B_f + \left[1 + \frac{h_t-x}{h-x}\right]\right\} \end{cases} \tag{6}$$

$$N_{st} = A_{st}E_s\epsilon_{ct} \tag{7}$$

$$N_R = bt_R E_R\epsilon_R \tag{8}$$

$$\epsilon_{ct} = \epsilon_R\frac{h-x}{h+0.5\,t_R-x} = \epsilon\frac{h-x}{h-x-a_t} = \epsilon_{cs}\frac{h-x}{x-a_c} = \epsilon_c\frac{h-x}{x} \tag{9}$$

where ε_{ct}, ε_R, ε_{ts}, ε_{cs}, and ε_c denote the strain at the bottom fiber of the T-section beam, strengthening plate, tensile reinforcement, compressive reinforcement, and top fiber of the T-section beam, respectively (see Figure 9); b and Bf denote the width of web and flange of the T-section beam, respectively; h_t, h_0, and h denote the depth of flange, effective depth, and overall depth of the cross-section, respectively.
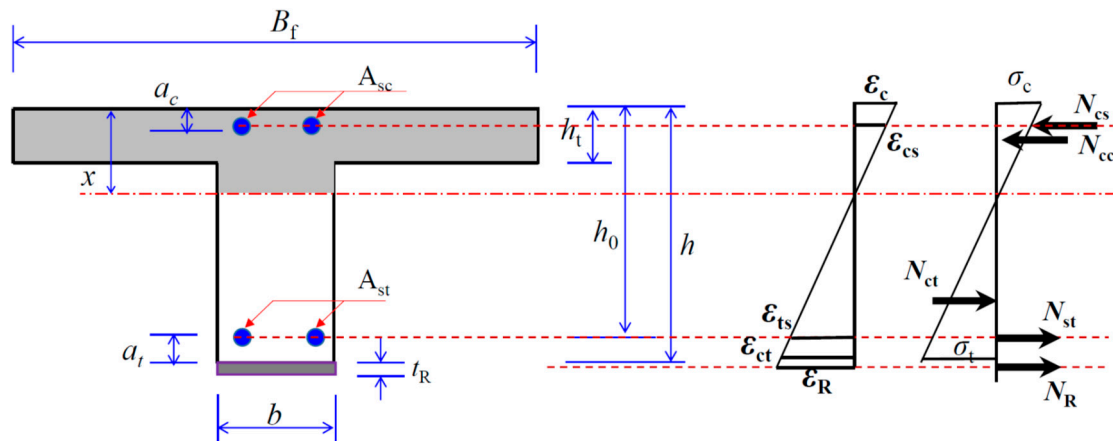
Figure 9. Strain and stress distribution on cross-section of T-section beam before concrete cracking.

Substituting the fracture strain $\varepsilon_{ct} = \varepsilon_{t0}$ into Equations (3)–(9), the neutral axis position, x, could be found. With x solved, the bending resistance of the cross-section could be determined through taking the moment to the neutral axis as follows;

$$M_{cR} = M_{cc} + M_{sc} + M_{st} + M_{ct} + M_R \tag{10}$$

$$M_{cc} = \left\{ \begin{array}{c} \frac{3x^2 - 3xh_1 + h_t^2}{3x} E_c \epsilon_c B_f h_t \\ \frac{2x^2}{3} E_c \epsilon_c B_f \end{array} \right\} \quad \left[\begin{array}{cc} for & x \geq h_t \\ \\ for & x < h_t \end{array} \right] \tag{11}$$

$$M_{sc} = E_s \epsilon_{cs} A_{sc} (x - a_c) \tag{12}$$

$$M_{st} = E_s \epsilon_{ct} A_{st} (h_0 - x) \tag{13}$$

$$M_{ct} = \left\{ \begin{array}{c} \frac{2}{3}(h-x)^2 b\sigma_t \\ \frac{h + h_t - 2x}{2(h-x)} \left[(h-x) - \frac{h + 2h_t - 3x}{3(h + h_t - 2x)}(h - h_1) \right] \epsilon_c E_c B_f \end{array} \right\} \quad \left[\begin{array}{cc} for & x \geq h_t \\ \\ for & x < h_t \end{array} \right] \tag{14}$$

$$M_R = E_R \epsilon_R A_R \left(h - x + \frac{t_R}{2} \right) \tag{15}$$

where σ_t denotes the ultimate tensile strength of the concrete A_{sc}, A_{st} and A_R denote the area of the compressive reinforcement, tensile reinforcement, and strengthening materials attached to the T-section beam. With the developed equations, the bending resistance of the cross-section can be determined. Thus, the resistance of the T-section beam corresponding to the crack initiation can be determined as follows:

$$P_{cr} = \frac{2M_{cr}}{L_a} \tag{16}$$

where L_a denotes the shear span of the beam.

6.2. Yielding Resistance and Ultimate Resistance of Strengthened T-Section Beams

The assumptions made to predict the yielding and ultimate resistance of the T-section beams strengthened by FRP include: (1) plane sections remain plane; (2) plastic stress was fully developed in the top fiber of the cross-section; (3) tensile strength of the concrete was ignored in the cross-section; and (4) the strengthening CFRP materials were assumed to be fully attached to the T-section beam. Figure 10 shows the strain and stress distributions in the cross-section corresponding to the yielding and ultimate resistance of the T-section beams. The position of the neutral axis in the cross-section could be found via equating the resultant internal forces acting on the cross-section to zero, i.e.,

$$N_{cc} + N_{sc} = N_{st} + N_R \tag{17}$$

$$N_{cc} = \left\{ \begin{array}{c} nf_cB_hh_t + nf_cb(\lambda x - h_t) \\ nf_cB_f\lambda x \end{array} \right\} \quad \left[\begin{array}{cc} for & x > h_t \\ for & x \leq h_t \end{array} \right] \tag{18}$$

$$N_{cs} = min\left(f_{yc}, E_s, \epsilon_{cs}\right)A_{sc} \tag{19}$$

$$N_{st} = min\left(f_{yt}, E_s, \epsilon_{ct}\right)A_{st} \tag{20}$$

$$N_R = bt_R\, min\,(f_R, E_R\epsilon_R) \tag{21}$$

$$\epsilon_{cu} = \epsilon_{ts}\frac{h-x}{h-x-a_t} = \epsilon_{cs}\frac{h-x}{x-a_c} = \epsilon_c\frac{h-x}{x} \tag{22}$$

where N_{cc}, N_{sc}, N_{st}, N_R, denote the internal resultant forces acting on the concrete under compression, compressive reinforcement, tensile reinforcement, and strengthening materials, respectively (see Figure 7); $\lambda = 0.8$ for fck ≤ 50 MPa, $\lambda = 0.8 - (\text{fck} - 50)/400$ for $50 < \text{fck} \leq 90$ MPa; $\eta = 1.0$ for fck ≤ 50 MPa; $\eta = 1.0 - (\text{fck} - 50)/200$ for $50 < \text{fck} \leq 90$ MPa [16]; B_f, b, h_t denote the width of the flange, width of the web, and height of the flange of the T-section beam, respectively; f_{yc}, f_{yt} denote the yield strength of the compressive and tensile steel reinforcement, respectively; A_{sc}, A_{st} and A_R denote the area of compressive reinforcement, tensile reinforcement, and strengthening CFRP attached to the T-section beam; h_t, h_0 denote the depth of flange, effective depth, and overall depth of the cross-section, respectively; ϵ_{cu} denotes the ultimate strain of the concrete under compression. Corresponding values for different strength of concrete could be determined as per the Eurocode 2 [16]. Thus, with the solved x, the plastic bending moment of the cross-section corresponding to yielding of the tensile reinforcement could be determined as follows;

$$M_{py} = M_{pc} + M_{psc} + M_{pst} + M_{pR} \tag{23}$$

$$M_{pc} = \left\{ \begin{array}{c} nf_cB_fh_t(x - 0.5h_t) + nf_c(\lambda x - h_t)b[x - h_t - 0.5(\lambda x \geq h_t)] \\ \lambda xnf_cB_f(x - 0.5\lambda x) \end{array} \right\} \quad \left[\begin{array}{cc} for & x \geq h_t \\ for & x < h_t \end{array} \right] \tag{24}$$

$$M_{psc} = min\left(f_{yc}, E_s\epsilon_{cs}\right)A_{sc}(x - a_c) \tag{25}$$

$$M_{pst} = min\left(f_{yt}, E_s\epsilon_{ct}\right)A_{st}(h_0 - x) \tag{26}$$

$$M_{pR} = bt_R min\,(f_R E_R\epsilon_R)\left(h - x + \frac{t_r}{2}\right) \tag{27}$$

where f_c denotes the compressive strength of the concrete.
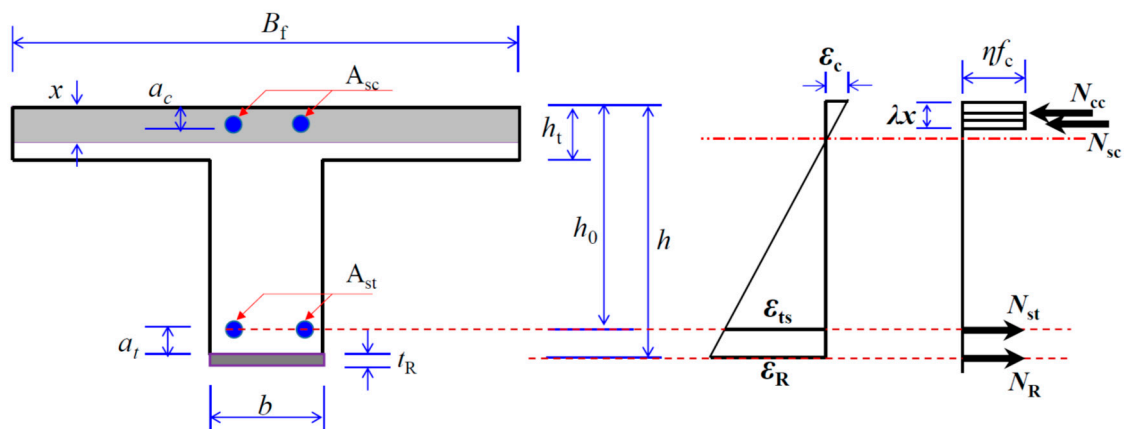

Figure 10. Strain and stress distribution on cross-section of T-section beams corresponding to yielding and ultimate resistance.

Regarding the bending resistance of the cross-section corresponding to the ultimate tensile strength of the flexural reinforcement M_{pu} the ultimate strength of the tensile steel reinforcement f_u can be used

for the calculation. Thus, the value of Equation (20) used in Equation (17) needs to be modified as follows:

$$N_{st} = min \ (f_{ut}, E_s \epsilon_{ct}) A_{st} \tag{28}$$

With the solved neutral axis position x in Equation (15), M_{pu} can be determined as follows:

$$M_{pu} = M_{pc} + M_{psc} + M_{pstu} + M_{pR} \tag{29}$$

$$M_{pstu} = min \ (f_{ut}, E_s \epsilon_{ct}) A_{st} (h_0 - x) \tag{30}$$

With the above developed equations, the bending resistance of the cross-section, M_{py} and M_{pu} can be determined. The load carrying capacity of the T-section beam corresponding to yield and ultimate strength of the flexural tensile reinforcement can be determined as follows:

$$P_y = \frac{2M_{py}}{L_a} \tag{31}$$

$$P_u = \frac{2M_{pu}}{L_a} \tag{32}$$

where La denotes the shear span of the beam. The predicted P_{cr}, P_y, and P_u values for the tested T-section beams are compared with the experimental values in Table 1. It can be observed that the developed analytical models predictions with reasonable accuracy for the resistance of the T-section beams strengthened by CFRP. The developed analytical models also provide reasonable prediction of the cracking resistance, yielding and ultimate resistance of the RC T-section beams strengthened with CFRP sheets. The average test-to-prediction ratio (or COVs) for P_{cr}, P_y, and P_u are 1.01 (0.12), 1.10 (0.12), and 1.08 (0.10), respectively.

7. Conclusions

This paper reports experimental results on the flexural behavior of RC T-section beams strengthened by CFRP sheets and proposes new analytical models to predict its behavior. Based on the test results, the failure mechanisms were analyzed, and the effects of various parameters were discussed. Robust analytical models were developed to predict the cracking resistance P_{cr}, yielding resistance P_y, and ultimate resistance P_u of the T-section beams strengthened by CFRP. Model accuracy was verified though validation against the experimental data. Based on the experimental and analytical study, the following conclusions can be drawn;

(1) The RC T-section beam specimens strengthened with CFRP sheets failed in a flexural failure. Increasing the thickness of the strengthening CFRP did not enhance the cracking resistance of the beam, but significantly improved the yielding and ultimate resistance.

(2) Increasing the flexural reinforcing ratio of the beam by 36% from 0.95% to 1.29% increased the P_{cr}, P_y, and P_u by 17%, 13%, and 48%, respectively.

(3) Increasing the CFRP U-wrap spacing had little effect on the resistance of the RC T-section beams. Moreover, increasing the compressive strength of concrete only had marginal influence on the yielding and ultimate resistance of the CFRP strengthened RC T-section beams.

(4) The T-section beams strengthened by CFRP sheets exhibited lower ductility at the final failure stage due to brittle failure of the bond between the CFRP sheet and concrete.

(5) The developed analytical models offered reasonable predictions of the cracking resistance, yielding and ultimate resistance of the RC T-section beams strengthened with CFRP sheets. The average test-to-prediction ratios (or COVs) for P_{cr}, P_y, and P_u were 1.01 (0.12), 1.10 (0.12), and 1.08 (0.10), respectively.

Conflicts of Interest: The authors have no conflict of interest related to this research publication.

References

1. Yubing, L. *The Field Investigation and Study of Concrete Bridge Structure*; Shenyang Jianzhu University: Shenyang, China, 2016; pp. 3–5.
2. Hui, P.; Jianren, Z.; Shouping, S. Experimental study of flexural fatigue performance of reinforced concrete beams strengthened with prestressed CFRP plates. *Eng. Struct.* **2016**, *127*, 62–72.
3. Esfahani, M.R.; Kianoushb, M.R.; Tajaria, A.R. Flexural behaviour of reinforced concrete beams strengthened by CFRP sheets. *Eng. Struct.* **2007**, *29*, 2428–2444. [CrossRef]
4. Arslan, G.; Sevuk, F.B.; Ekiz, I. Steel plate contribution to load-carrying capacity of strengthened RC beams. *Constr. Build. Mater.* **2008**, *22*, 143–153. [CrossRef]
5. Hadjazi, K.; Sereir, Z.; Amziane, S. Creep response of intermediate flexural cracking behavior of reinforced concrete beam strengthene d with an externally bonde d FRP plate. *Int. J. Solids Struct.* **2016**, *94*, 196–205. [CrossRef]
6. Hugo, C.; Biscaia, C.; Chastre, M.; Silva, A.G. A smeared crack analysis of reinforced concrete T-section beams strengthened with GFRP composites. *Eng. Struct.* **2013**, *56*, 1346–1361.
7. Carvalho, T.; Chastre, C.; Biscaia, H.; Paula, R. Flexural behaviour of RC T-section beams strengthened with different FRP materials. In *Third International Fib Congress*; Fib: Lausanne, Switzerland; Washington, DC, USA, 2010.
8. Ascione, L.; Feo, L. Modeling of composite/concrete interface of RC beams strengthened with composite laminates. *Compos. Part B Eng.* **2000**, *31*, 535–540. [CrossRef]
9. Bonacci, J.F.; Maalej, M. Behavioral trends of RC beams strengthened withexternally bonded FRP. *J. Compos. Constr.* **2001**, *5*, 102–113. [CrossRef]
10. Badawi, M.; Soudki, K. Flexural strengthening of RC beams with prestressed NSM CFRP rods: Experimental and analytical investigation. *Constr. Build. Mater.* **2009**, *23*, 3292–3300. [CrossRef]
11. Al-Mahmoud, F.; Castel, A.; François, R.; Tourneur, C. Strengthening of RC members with near-surface mounted CFRP rods. *Compos. Struct.* **2009**, *91*, 138–147. [CrossRef]
12. Yost, J.R.; Gross, S.P.; Dinehart, D.W.; Mildenberg, J.J. Flexural behavior of concrete beams strengthened with near-surface-mounted CFRP strips. *Aci. Struct. J.* **2007**, *104*, 430–437.
13. Bilotta, A.; Ceroni, F.; Di Ludovico, M.; Nigro, E.; Pecce, M.; Manfredi, G. Bond efficiency of EBR and NSM FRP systems for strengthening concrete members. *J. Compos. Constr.* **2011**, *15*, 757–772. [CrossRef]
14. Barros, J.A.O.; Fortes, A.S. Flexural strengthening of concrete beams with CFRP laminates bonded into slits. *Cem. Concr. Compos.* **2005**, *27*, 471–480. [CrossRef]
15. Nanni, A.; Ludovico, D.M.; Parretti, R. Shear strengthening of a PC bridge girder with NSM CFRP rectangular bars. *Adv. Struct. Eng.* **2004**, *7*, 297–309. [CrossRef]
16. EN. B. 1-1. *Eurocode 2. Design of Concrete Structures—Part 1-1: General Rules and Rules for Buildings*; Eur. Comm. Stand.: Dublin, Ireland, 2004; 277p.